CYBERNETICS AND PHYSICS, VOL. 2, NO. 1, 2013 , 5–9

MODELING AND SYNCHRONIZATION OF MULTIVIBRATOR OSCILLATORS

Leonardo Acho
CoDAlab, Departament de Matemàtica Aplicada III,
Escola Universitària d'Enginyeria Tècnica Industrial de Barcelona,
Universitat Politècnica de Catalunya
SPAIN
leonardo.acho@upc.edu

Abstract

In this work we present a mathematical modeling of astable (or free-running) multivibrator oscillators. Then, using this model, we develop an algorithm to synchronize two multivibrator oscillators. Lyapunov's theory is employed to validate our design. Numerical and experimental results are given to support our findings.

Key words

Multivibrator oscillators, modeling, synchronization.

1 Introduction

A multivibrator system is an electronic circuit that switches rapidly by means of positive feedback between two states. There are three types of multivibrator circuits depending on its realization: astable, monostable, and bistable. Here, we are interested in the *astable* multivibrators, also called *free-running* multivibrators, because they are used in some timing event devices, and they can be set by a suitable and simple electronic network [Franco, 2002]. These oscillators are not stable in either state (it continually switches from one state to the other). Moreover, these devices do not require an input such as a clock pulse.

From the mathematical modeling point of view, a mathematical representation able to capture the periodic behavior of astable multivibrators is an important issue to study them. On the other hand, this mathematical representation can be employed, for instance, to design a synchronization algorithm between two astable multivibrators, among other topics. To the best author acknowledgement, a practical mathematical model of astable multivibrator systems has not been released.

Synchronization can be understood as the coordination of events to operate a system in unison. Oscillators synchronization is an important issue, for instance, in some synthesizers with two or more voltage-controller-oscillator. Or to synchronize digital devices that are sharing data, and so on. Moreover, and according to [Dodla, Sen and Johnston, 2003], *coupled* limit cycle oscillators (a kind of synchronization) have been studied to understand synchronization phenomena in various physical, chemical, and biological systems. Another instance is the mutual synchronization of interacting oscillators which has been observed in all fields of physics [Klinshov, 2012]. Finally, synchronization of chaotic oscillators has been extensively studied (to name a few, see [Chen, 2005], [Feki, 2009], [Tan, Zhang and Yang, 2003], and [Kuntanapreeda and Sangpet, 2012]). So, synchronization is a topic to learn more about systems.

Here, we use our mathematical model to synchronize two free-running multivibrator oscillators. We prefer to use the master-slave approach because this approach has been extensively used. The proposed synchronization scheme is validated by invoking Lyapunov's theory. Moreover, numerical and experiential results are granted to support our findings. In resume, the contributions of this paper are modeling and synchronization of free-running multivibrator oscillators.

The rest of the this work is structured as follows. Section 2 shows analysis and modeling of free-running multivibrator oscillators. A numerical simulation is granted to support our mathematical model. Section 3 is dedicated to the synchronization problem statement and a solution to it using Lyapunov's theory and our mathematical model. Numerical experiments are given too. Experimental results are realized in Section 4. Finally, conclusions are stated in Section 5.

2 Astable Multivibrator Oscillators: Analysis and Modeling

The basic free-running multivibrator circuit is shown in Fig. 1 [Franco, 2002]. Although the 301 operational amplifier (*op-amp*) is preferred for this kind of application, we use the traditional LM741 op amp (see Section five). In the circuit, the op-amp has a positive-feedback resistances R_1 and R_2 forming an inverting Schmitt trigger configuration. This positive-feedback produces *toggles* between one state (when $V_o = V_{SAT}$) and the other (when $V_0 = -V_{SAT}$). See Fig. 2. This because the positive-feedback increases the op-amp gain, which helps to toggle very fast between these states. The capacitor C is connected to the non-inverting input of the op-amp with its other end connected to ground. This capacitor, together with the resistance R, form a RC integrator. This RC integrator controls the timing of the system [1]. From the circuit, we have $\pm Vp = \pm V_o(\frac{R_2}{R_1+R_2}) = \pm V_{SAT}(\frac{R_2}{R_1+R_2})$.

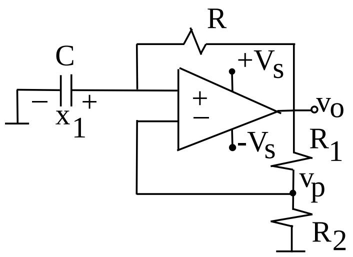

Figure 1. Basic astable multivibrator circuit.

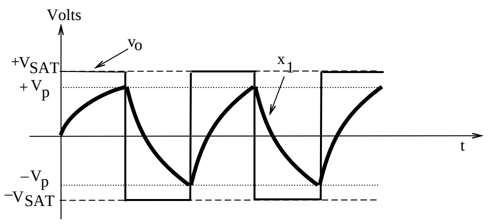

Figure 2. Waveforms for the free-running multivibrator ($\pm V_{SAT}$ are the saturating voltages).

Let $x_1 := x_1(t)$ be the capacitor voltage, and assume that $| x_1(0) | < Vp$ (this assumption is a realistic one because when the circuit is initially power on, this initial condition is very close to zero). The waveform $x_1(t)$ is also shown in Fig.2. Then, and from Fig. 2, the operation of the astable multivibrator can be summarized as follows.

1) If $| x_1(t) | \leq V_p$ and $\dot{x}_1 > 0$, then

$$\dot{x}_1 = \alpha(-x_1 + V_{SAT}), \tag{1}$$

2) if $| x_1(t) | \leq V_p$ and $\dot{x}_1 < 0$, then

$$\dot{x}_1 = \alpha(-x_1 - V_{SAT}), \tag{2}$$

3) if $| x_1(t) | > V_p$ and $\dot{x}_1 > 0$, then

$$\dot{x}_1 = \alpha(-x_1 - V_{SAT}), \tag{3}$$

and

4) if $| x_1(t) | > V_p$ and $\dot{x}_1 < 0$, then

$$\dot{x}_1 = \alpha(-x_1 + V_{SAT}), \tag{4}$$

where $\alpha = \frac{1}{RC}$. Combining (1) and (2), yields:

a) if $| x_1(t) | \leq V_p$, then

$$\dot{x}_1 = \alpha(-x_1 + V_{SAT} sgn(\dot{x}_1)). \tag{5}$$

And combining (3) and (4), we have:

b) if $| x_1(t) | > V_p$, then

$$\dot{x}_1 = \alpha(-x_1 - V_{SAT} sgn(\dot{x}_1)), \tag{6}$$

where $sgn(\cdot)$ is the signum function.

Finally, combining (5) and (6), we obtain:

$$\dot{x}_1 = \alpha(-x_1 - V_{SAT} sgn(\dot{x}_1) sgn(| x_1 | - V_p)) \ , \quad | x_1(0) | < V_p. \tag{7}$$

The system (7) has the disadvantage that the right hand-side depends on $\dot{x}_1$. One option to avoid it is to use the system shown Fig. 3 to estimate time derivatives [2]. If a is too small, then the block diagram shown in Fig. 3 will be similar to a differentiator. Using the state space representation of the system in Fig. 3, together with (7), we arrive to the next dynamic model of the astable multivibrator oscillator able to capture the evolution of $x_1(t)$ similar to the one shown in Fig. 2:

$$\dot{x}_1 = \alpha(-x_1 - V_{SAT} sgn(y_1) sgn(| x_1 | - V_p)), \quad | x_1(0) | < V_p \tag{8}$$

$$\dot{z_1} = -\frac{1}{a}(z_1 + x_1), \tag{9}$$

$$y_1 = \frac{1}{a}(z_1 + x_1). \tag{10}$$

Fig. 4 shows a simulation result of the system (8)-(10) with $\alpha = 0.1$, $V_p = 1$, $V_{SAT} = 2$, and $a = 0.01$.

[1] A formula to estimate the oscillation frequency is [Franco, 2002]: $f = \frac{1}{2RCln(1+2R_1/R_2)}$.

[2] There are other transfer functions to estimate the derivative of a signal, but we prefer the one shown in Fig. 3 because its simplicity.

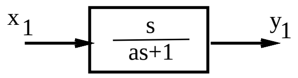

Figure 3. A time derivative estimator: s is the Laplace's variable.

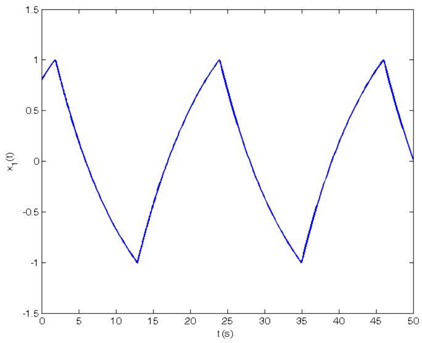

Figure 4. Simulation result ($x_1(0) = 0.8$ and $z_1(0) = 0$).

3 Synchronization Design

Consider the driven (or master) system given by (8)-(10), and conceive the following receiver (or slave) system:

$$\dot{x}_2 = \alpha(-x_2 - V_{SAT} sgn(y_2) sgn(\mid x_2 \mid -V_p)) + u, \quad \mid x_2(0) \mid < V_p \tag{11}$$

$$\dot{z}_2 = -\frac{1}{a}(z_2 + x_2), \tag{12}$$

$$y_2 = \frac{1}{a}(z_2 + x_2), \tag{13}$$

where u is the control input to be designed such that the next synchronization objective is satisfied:

$$\lim_{t \to \infty} x_2(t) = x_1(t). \tag{14}$$

By defining the synchronization error $e(t) = x_2(t) - x_1(t)$, and using the Lyapunov function:

$$V(t) = \frac{1}{2}e^2, \tag{15}$$

its time derivative along the system trajectories (8)-(10) and (11)-(12), yields,

$$\dot{V}(t) \leq -\alpha e^2 + e(u + 2\alpha). \tag{16}$$

Designing:

$$u = -ksgn(e) = -ksgn(x_2(t) - x_1(t)), \quad k > 2\alpha, \tag{17}$$

we obtain $\dot{V}(t) \leq -\alpha e^2$, implying that our synchronization objective is satisfied. In resume, we have the following result.

Theorem 1. *Given the master system (8)-(10), and the slave system (11)-(12); utilizing the control algorithm (17), the synchronization objective (14) is satisfied.*

Figure 5 shows numerical results of the synchronization process using $\alpha = 0.1$, $V_p = 1$, $V_{SAT} = 2$, $a = 0.01$, $k = 1$, and $x_1(0) = 0.8$ and $x_2(0) = -0.8$ ($z_1(0) = z_2(0) = 0$).

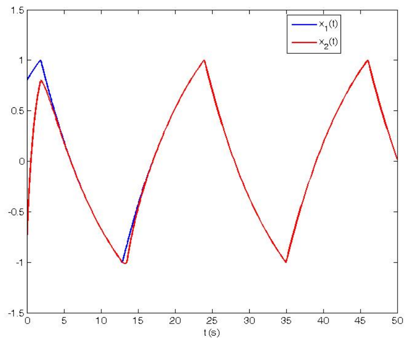

Figure 5. Simulation result of the synchronization process.

4 Experimental Results

For the experimental evaluation of our theoretical findings, we built the electronic circuit show in Fig. 6. The circuit is realized using $R_1 = R_2 = R = 1k\Omega$, and $C = 220\mu F$. In this figure, we have the master and slave systems, and the synchronization control law realized using the third op-amp in open-loop connection. In this configuration, this op-amp will produce the control law (17) with its maximum possible value of $k (= V_{SAT})$, but is it applied to the slave system as follows:

$$\dot{x}_2 = \alpha(-x_2 - ksgn(x_2 - x_1)). \tag{18}$$

Using the same Lyapunov function $v(t) = \frac{1}{2}e^2$, with $e = x_2 - x_1$, its time derivative along the system trajectories (8)-(10) and (18), yields:

$$\dot{V}(t) \leq -\alpha e^2 - \alpha \mid e \mid (k - 1). \tag{19}$$

So, if $k > 1$, then $\dot{V}(t) \leq -\alpha e^2$, satisfying the synchronization objective (14).

In our circuit, all operational amplifiers are the LM741 integrated circuits. The capacitor $C_x = 0.033\mu F$[3] is employed to filter corrupted signals . Figure 7 shows

[3] In our experiment, this capacitor seems unnecessary. But, it is correct to use it.

a picture of the circuit shown in Figure 6. We use the *PicoScope* PC oscilloscope software to capture the output signals ($V_o's$) on both systems, the master and the slave systems. This PicoScope device is connected to a Laptop (see Fig. 8). Figure 9 shows these output signals when the synchronization control law is inactive. Figure 10 displays the experimental result when the synchronization control law is activated.

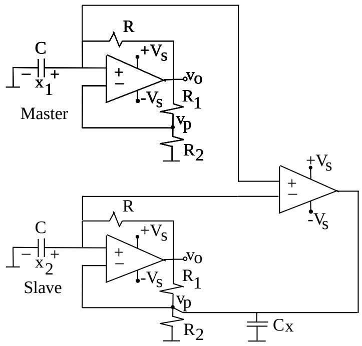

Figure 6. Electronic circuit.

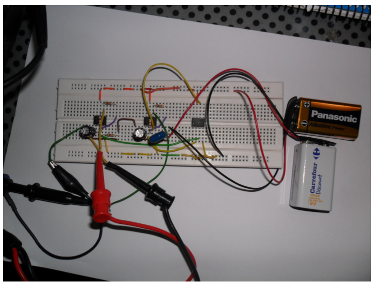

Figure 7. A picture of the circuit realization.

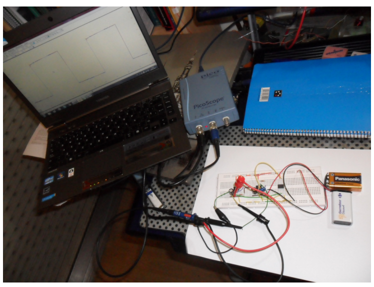

Figure 8. A picture of the experiment set-up.

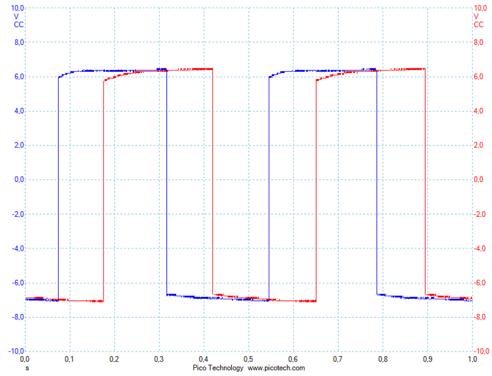

Figure 9. Experimental result of the system without the synchronization control law (blue-line is the master's output, and red-line is the slave's output).

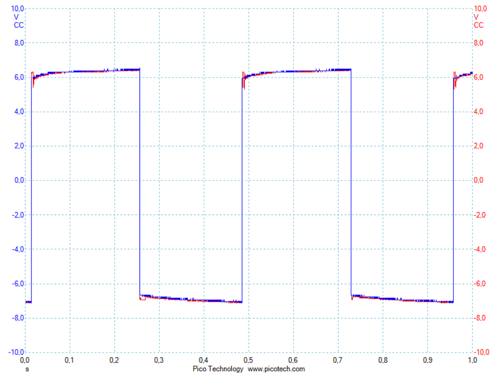

Figure 10. Experimental result of the system with the synchronization control law activated (blue-line is the master's output, and red-line is the slave's output).

5 Conclusions

This paper has introduced a mathematical model of free-running multivibrator oscillators together with a simple synchronization algorithm to synchronize two astable multivibrator oscillators. Using this synchronization algorithm, an experimental circuit realization of it was possible.

Acknowledgements

This work was supported by the Spanish Ministry of Economy and Competitiveness under Grant number DPI2012-32375.

References

Chen, H.(2005) Global chaos synchronization of new chaotic systems via nonlinear control. *Chaos, Solitons, and Fractals*, **23**, pp. 1245–1251.

Dodla, R., Sen, A., and Johnston, G.(2003) Driven response of time delay coupled limit cycle oscillators.

Commun. in Nonlinear Science and Numerical Simulation, **8**, pp. 493–518.

Feki, M.(2009) Sliding mode control and synchronization of chaotic systems with parametric uncertainties. *Chaos, Solitons, and Fractals*, **41**, pp. 1390–1400.

Franco, S.(2002) *Design with operational amplifiers and analog integrated circuits*. McGraw-Hill,3 th Edition.

Klinshov, V., and Nekorkin, V.(2012) Synchronization in networks of pulse oscillators with time-delay coupling. *Cybernetics and Physics*, **1**, pp. 106–112.

Kuntanapreeda, S. and Sangpet, T.(2012) Synchronization of chaotic systems with unknown parameters using adaptive passivity-based control. *Journal of the Frankling Institute*, **349**, pp. 2547–2569.

Tan, X., Zhang, J., and Yang, Y.(2003) Synchronizing chaotic systems using backstepping design. *Chaos, Solitons, and Fractals*, **16**, pp. 37–45.